View metadata, citation and similar papers at core.ac.uk
brought to you by CORE
provided by Archivio istituzionale della ricerca - Politecnico di Milano

Hydrophobin as a Nanolayer Primer That Enables the Fluorinated Coating of Poorly Reactive Polymer Surfaces

Lara Gazzera, Claudio Corti, Lisa Pirrie, Arja Paananen, Alessandro Monfredini, Gabriella Cavallo, Simona Bettini, Gabriele Giancane, Ludovico Valli, Markus B. Linder, Giuseppe Resnati,* Roberto Milani,* and Pierangelo Metrangolo**

A new and simple method is presented to fluorinate the surfaces of poorly reactive hydrophobic polymers in a more environmentally friendly way using the protein hydrophobin (HFBII) as a nanosized primer layer. In particular, HFBII, via electrostatic interactions, enables the otherwise inefficient binding of a phosphate-terminated perfluoropolyether onto polystyrene, polypropylene, and low-density polyethylene surfaces. The binding between HFBII and the perfluoropolyether depends significantly on the environmental pH, reaching the maximum stability at pH 4. Upon treatment, the polymeric surfaces mostly retain their hydrophobic character but also acquire remarkable oil repellency, which is not observed in the absence of the protein primer. The functionalization proceeds rapidly and spontaneously at room temperature in aqueous solutions without requiring energy-intensive procedures, such as plasma or irradiation treatments.

1. Introduction

The surface modification of polymers is often essential to achieve control over important interface features without changing the bulk properties of the polymer as the process is usually achieved using only limited amounts of a surface modifier. In particular, introducing fluorocarbon moieties on a polymer surface plays a key role in improving its performances in terms of chemical resistance, friction reduction, and barrier and antireflection properties, among others, as well as preparing easy-to-clean, omniphobic, and low-energy surfaces.[1–5]

The most straightforward strategy toward fluorocarbon-coated surfaces consists of the simple physical deposition of a fluoropolymer film.[3] However, this approach necessitates a rather thick film to achieve significant durability and, therefore, requires a relatively large amount of fluoropolymer. Alternative approaches, such as chemical grafting of fluoropolymers by radical methods through irradiation,[6–8] plasma,[9–12] or direct fluorination with fluorine gas,[1,2,13] require only moderate amounts of fluorinated surface modifiers but are much more aggressive and, in some cases, potentially hazardous.

Other possibilities involve functionalization with fluorinated molecules/polymers consisting of specific chemical moieties that are able to bind either covalently or noncovalently to the polymer surface.[4,5,14,15] However, to achieve sufficiently stable bonding, this general strategy requires the presence of reactive hydrophilic sites, typically —OH groups, which are not typically observed on the surfaces of apolar, hydrophobic polymers, such as polyolefins, and need to be introduced via oxidizing pretreatments that are usually either energy-intensive or not environmentally friendly.[16–19] Expanding on this strategy, we present an efficient, rapid, and more environmentally friendly method to perform the fluorocarbon coating of hydrophobic polymer surfaces. The method is based on the use of hydrophobins, i.e., amphiphilic surface-active proteins, as a nanosized primer layer that adheres to the hydrophobic polymer surface, making the surface hydrophilic and preparing it for the subsequent binding of a fluoropolymer containing ionic moieties.

Hydrophobins are a class of nontoxic, surface-active, and film-forming proteins that are produced by filamentous

Dr. L. Gazzera, C. Corti, Dr. L. Pirrie, A. Monfredini,
Prof. G. Cavallo, Prof. G. Resnati, Prof. P. Metrangolo
Laboratory of Nanostructured
Fluorinated Materials (NFMLab)
Department of Chemistry
Materials and Chemical Engineering "Giulio Natta"
Politecnico di Milano
Via Mancinelli 7, I-20131 Milan, Italy
E-mail: giuseppe.resnati@polimi.it; pierangelo.metrangolo@polimi.it
Dr. A. Paananen, Dr. R. Milani
VTT-Technical Research Centre of Finland
Biologinkuja 7, Espoo, P.O. Box 1000 FI-02044 VTT, Finland
E-mail: roberto.milani@vtt.fi
Dr. S. Bettini, Dr. G. Giancane, Prof. L. Valli
Università del Salento
Centro Ecotekne Pal. O – S.P. 6
Lecce – Monteroni –, LECCE 73100, Italy
Prof. M. B. Linder
School of Chemical Technology
Aalto University
Kemistintie 1, P.O. Box 16100 FI-00076 Aalto, Espoo, Finland
E-mail: markus.linder@aalto.fi
Prof. G. Resnati, Prof. P. Metrangolo
Center for Nano Science and Technology@Polimi
Istituto Italiano di Tecnologia
via Giovanni Pascoli, 70/3, Milano 20133, Italy

This is an open access article under the terms of the Creative Commons Attribution-NonCommercial-NoDerivatives License, which permits use and distribution in any medium, provided the original work is properly cited, the use is non-commercial and no modifications or adaptations are made.

DOI: 10.1002/admi.201500170

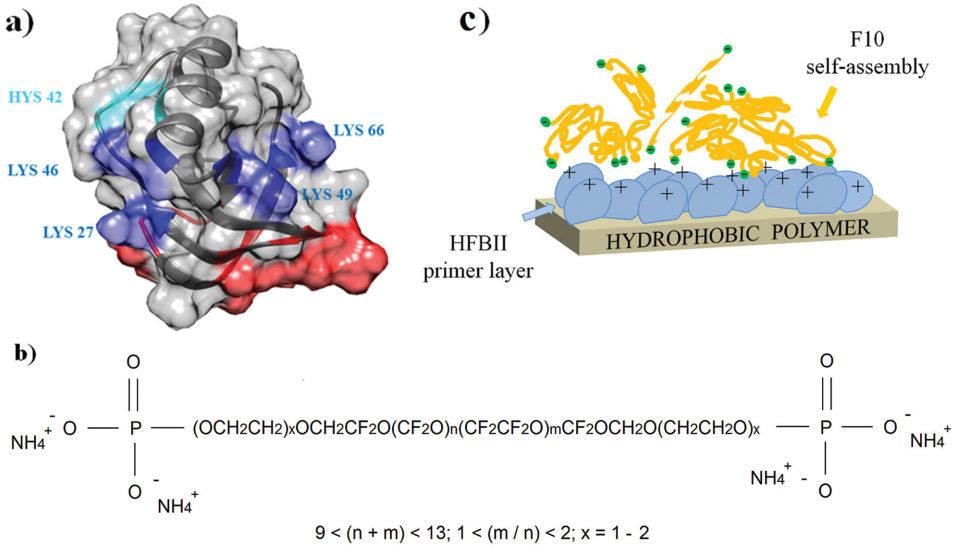

Figure 1. a) Structure of the HFBII protein with the hydrophobic patch highlighted in red and the positively charged amino acids highlighted in blue (Lys) and light blue (Hys); b) chemical formula of Fluorolink F10; c) schematic representation of the interaction expected between F10 and a layer of HFBII deposited onto an apolar polymer surface.

fungi.[20] The presence of eight cysteine residues arranged in four internal disulfide bridges[21] significantly enhances the resistance of these proteins to both heat and organic solvents. Most importantly, a discrete portion of their exposed surface is composed of amino acids with hydrophobic side-chains; this hydrophobic patch endows hydrophobins with exceptional amphiphilic properties and drives their spontaneous and rapid self-assembly at hydrophobic/hydrophilic interfaces, such as air/water and oil/water boundaries, where they pack into ordered structures and form remarkably strong and elastic films.[22,23] Hydrophobins also efficiently assemble onto solid surfaces to form amphiphilic films that are able to reverse the surface wettability of the coated material[24] and allow for the immobilization of, e.g., proteins or enzymes onto solid surfaces[25–28] while preserving all of the features of the immobilized biomolecules.[29] The main advantage of this method is its simplicity: hydrophobin self-assembly proceeds spontaneously at room temperature within seconds or minutes and requires only a very tiny amount of protein. Moreover, hydrophobins are natural, edible, and nontoxic surface modifiers that can be deposited from aqueous solutions, significantly increasing the sustainability of the entire process.

In the present work, we focused on the class II hydrophobin HFBII, a 7.2 kDa hydrophobin from *Trichoderma reesei* that possesses a globular structure (**Figure 1**a). The dimensions of the protein are 2.4 × 2.7 × 3.0 nm, as derived from its single crystal X-ray structure,[30] with a hydrophobic patch of approximately 4 nm^2. HFBII was used as a nanosized primer layer to mediate the otherwise inefficient binding of the phosphate-terminated perfluoropolyether (PFPE) Fluorolink F10 (henceforth abbreviated as F10) onto various hydrophobic polymer surfaces, such as those of polystyrene (PS), polypropylene (PP), and low-density polyethylene (LDPE). The selection of F10, a PFPE, as a surface modifier is motivated by the better environmental compliance of this class of compounds compared with long-chain perfluoroalkanes: PFPE chains are biocompatible[31–35] and less persistent while still being substantially inert from the chemical viewpoint. The protein was expected to adhere spontaneously to the polymer surface through its hydrophobic patch while exposing hydrophilic amino acids bearing ionizable side chains. Among these are the Lys residues in positions 27, 46, 49, and 66, and the Hys residue in position 42, which are able to interact electrostatically with the phosphate groups of F10 (Figure 1b). We demonstrated this two-step self-assembly process on a model hydrophobic surface using a quartz crystal microbalance with dissipation monitoring (QCM-D), contact angle measurements (CA), and atomic force microscopy (AFM) imaging. Subsequently, we successfully extended this same coating strategy to the surfaces of commercial samples of PS, PP, and LDPE, significantly reducing their oleophilic character.

2. Results and Discussion

F10 is a PFPE with a linear chain structure, bearing oligoethylene glycol portions at the extremities capped with ammonium phosphate end groups that may be used to establish electrostatic interactions with the protein primer layer. HFBII features five positively charged amino acids on the exposed hydrophilic side,[21,36,37] and its isoelectric point (pI) was measured to be 5.8 (see Figure S1 and Table S1 of the Supporting Information). Therefore, the hypothesized interaction between HFBII and F10 was expected to be electrostatic and pH dependent. The best binding conditions should occur below the pI of the protein, where HFBII becomes positively charged. However, excessive lowering of the pH would result in protonation of the phosphate groups, thus weakening the electrostatic attraction between the two components.

For this reason, we first studied the pH-dependent self-assembly process by QCM-D, using a self-assembled monolayer (SAM) of octadecylmercaptan on a gold sensor as a model for a hydrophobic polymer surface. Control experiments

© 2015 The Authors. Published by WILEY-VCH Verlag GmbH & Co. KGaA, Weinheim

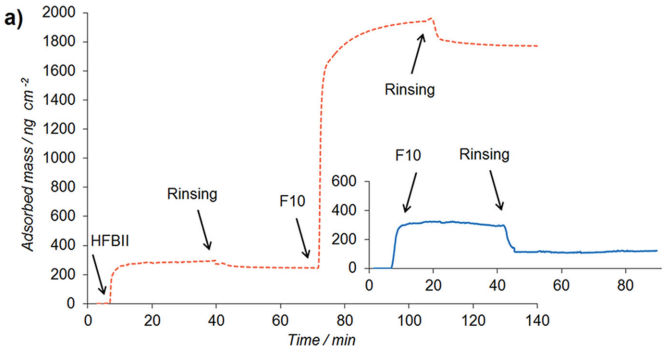

b)

pH	HFBII adsorbed mass [ng cm^{-2}]	TOTAL adsorbed mass [ng cm^{-2}]
3	206	920
	-	102
4	246	1772
	-	118
5	247	426
	-	55
6	243	285
	-	46
8	217	220
	-	31

Figure 2. a) Adsorbed mass (ng cm^{-2}) of F10 at pH 4 with (orange dashed line) and without (blue continuous line) the deposition of an HFBII primer layer; b) calculated values of the adsorbed mass (ng cm^{-2}) of the first HFBII layer and after the subsequent deposition of F10 on gold sensors coated with an octadecylmercaptan SAM, as derived from the QCM-D measurements. The data also include control experiments performed without an HFBII primer layer.

were performed to evaluate the different adhesion capabilities of HFBII and F10 on the hydrophobic surface.

2.1. Binding Studies on Model Surfaces

The experimental surface coverage density of HFBII on the hydrophobic SAM was close to 250 ng cm^{-2} at pH 4 and 6, which is in good agreement with the value of 240 ng cm^{-2} observed for a monolayer of HFBI, another class II hydrophobin structurally similar to HFBII.[38] Therefore, it was assumed that HFBII also formed monolayers under these conditions. Furthermore, the overlapping of all of the measured frequency harmonics, combined with the low dissipation increase, demonstrated that the protein film exhibited an essentially rigid behavior, which is likely associated with a fairly efficient packing of the protein into a dense monolayer.

Based on the QCM-D response of the F10 control sample, only a very tiny amount of F10 bound weakly to the model hydrophobic surface at every pH in the absence of the HFBII primer layer (**Figure 2**b; the complete dataset is presented in Figure S2 and Table S2 of the Supporting Information). In fact, most of the PFPE (from 33 to 63%, depending on the environmental pH) was removed from the sensor surface upon rinsing.

In contrast, the presence of a primer layer of HFBII assembled onto the hydrophobic sensor significantly improved the binding of F10 at pH < pI. The largest amount of F10 bound to the HFBII-coated sensor surface at pH 4 (Figure 2, the complete dataset is presented in Figure S3 and Table S2 of the Supporting Information), where the molar ratio between the two assembled components was calculated to be approximately 30:1. This result implies that the positively charged HFBII-coated surface attracts the negatively charged micellar aggregates that F10 is known to form in aqueous solution.[39–41] Smaller amounts of F10 were adsorbed at pH 3 and 5, while drastic mass decreases were observed at pH values close to and higher than the pI of HFBII. In particular, only a negligible amount of F10 was adsorbed in the experiment performed at pH 8, thus confirming the repulsive effect expected when both the protein and the PFPE are negatively charged (see Figure S3e of the Supporting Information). Furthermore, the effective binding of F10 resulted in a significant increase in the dissipation factor *D* with a simultaneous splitting of the frequency overtones (see Figure S3b of the Supporting Information), thus suggesting a more viscoelastic behavior than the HFBII layer, which is consistent with the amorphous character of PFPEs.

2.2. Binding Studies on Polystyrene Surfaces

QCM-D experiments were also performed at pH 4 on PS-coated sensors, which confirmed the fact that the protein primer is essential for the stable binding of F10 on this surface (Figure S4 of the Supporting Information). Similar to the model SAM system, HFBII bound to the PS surface as an approximate monolayer (≈280 ng cm^{-2}) and enabled the subsequent binding of about 1330 ng cm^{-2} of F10 onto the surface. For comparison, the amount of adsorbed PFPE on the PS surface in the absence of HFBII was only about 70 ng cm^{-2}. The adsorbed PFPE:HFBII molar ratio in this case was calculated to be approximately 23:1, which is in fair agreement with that observed for the model SAM system and supports a similar hypothetical binding of F10 aggregates rather than individual molecules.

The presence of the HFBII primer layer thus ensures a stable PFPE coating, as also demonstrated by the much lower F10 desorption during the washing step compared with the control samples prepared without the intermediate protein layer (see Table S2 of the Supporting Information). In addition, the observed pH dependency suggests that the binding mainly occurs through electrostatic interactions, as hypothesized.

2.3. Performance Evaluation of the Coated Model Surfaces

Interesting findings were obtained from static contact angle (CA) measurements on the coated sensors prepared during the QCM experiments (see Table S3 of the Supporting Information). The presence of HFBII reversed the wettability of the hydrophobic SAM, making it more hydrophilic, as was planned. The water CA of the octadecylmercaptan SAM decreased from 109° to approximately 60° after the deposition of an HFBII layer independent of the pH, thus suggesting that the protein

 © 2015 The Authors. Published by WILEY-VCH Verlag GmbH & Co. KGaA, Weinheim

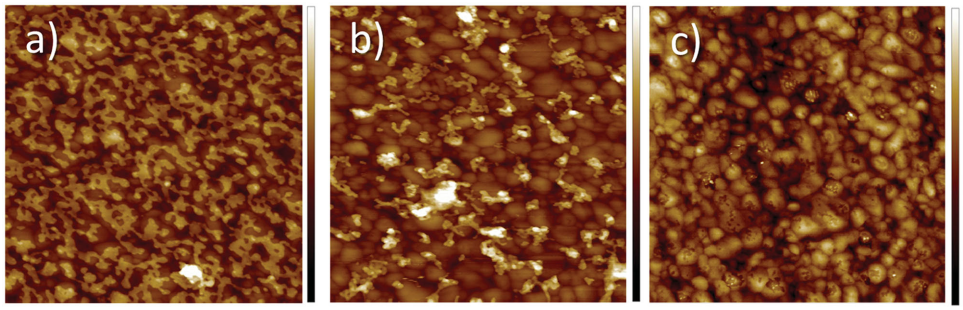

Figure 3. AFM topography images of a) an HFBII film, b) a HFBII + F10 film, and c) octadecylmercaptan SAM on a gold chip. The films were deposited on (c) at pH 4 in QCM-D experiments. The area displayed in each image is 1 × 1 μm, and the height color scale (black to white) spans 15 nm in (a), 25 nm in (b), and 10 nm in (c).

binding mechanism does not involve charged residues, as expected, and increased back to ≈112° after the subsequent F10 binding. More notably, the dodecane CA increased to 58° from 26° of the pristine SAM for the sensor surface prepared at pH 4 by subsequent self-assembly of HFBII and F10. This finding demonstrates that this approach can substantially decrease the oleophilicity of the surface.

The sensor surfaces prepared during the QCM-D experiments at pH 4 were also imaged by AFM to characterize the morphology of the deposited films. **Figure 3**a shows a dried film of HFBII on the sensor surface coated with the hydrophobic SAM. It appears that the HFBII does not fully cover the underlying SAM surface as a monomolecular layer and instead forms islets of average thickness above one monolayer. This hypothesis is supported by the fact that the observed thickness of the protein layer varied between 2 and 5 nm, while the dimensions of the HFBII protein are approximately 2–3 nm. The RMS roughness S_q of the protein-coated surface was 2.57 ± 0.17 nm, which is expectedly higher than that of the simple octanethiol SAM reported in Figure 3c (1.27 ± 0.06 nm). By contrast, Figure 3b shows the SAM-coated sensor surface after subsequent deposition of HFBII and F10. Worm-like aggregates of HFBII/F10 that reach up to 20 nm in height are distributed over the SAM surface, resulting in partial coverage and further increased roughness (S_q = 2.96 ± 0.24 nm). These aggregates are able to confer stable oil-repellency to the SAM surface, as demonstrated by QCM and CA measurements.

2.4. Coating Studies of Commercial Polymer Surfaces

To demonstrate the effectiveness, generality, and scalability of our method, we decided to apply it to the surface of commercially available PS, PP, and LDPE sheets. The samples were prepared by dipping the polymer sheets in sequence into aqueous solutions of HFBII and F10, both buffered at pH 4, which afforded the best deposition conditions according to the model studies.

The effective binding of the protein and PFPE to the surfaces of the LDPE samples was demonstrated by attenuated total reflectance (ATR) FT-IR spectroscopy (**Figure 4**; for the complete FT-IR spectra of HFBII and F10, see Figures S5 and S6 of the Supporting Information). In particular, the conserved HFBII amide I and II peaks are clearly identifiable in the region between 1720 and 1450 cm^{-1} (Figure 4a), while the presence of F10 is revealed by the characteristic C–F stretching peaks in the region between 1400 and 1000 cm^{-1} (Figure 4b). Importantly, no such peaks were detectable in the LDPE samples treated only with the PFPE without the protein primer layer, thus confirming the key role of HFBII in determining the stable deposition of F10 onto hydrophobic polymeric surfaces. Unlike LDPE,

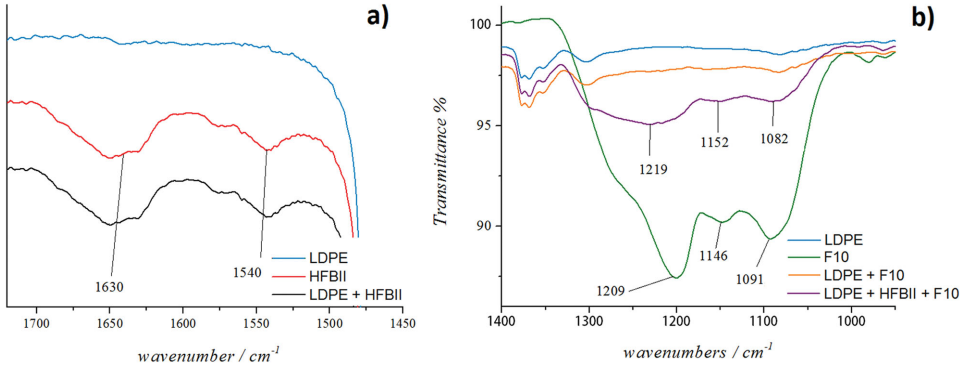

Figure 4. ATR-FT-IR magnified and superimposed spectra of a) pristine LDPE (sky blue), pure HFBII (red), and LDPE coated with HFBII (black) between 1720 and 1450 cm^{-1}; b) pristine LDPE (sky blue), pure F10 (green), and LDPE treated with F10 with the HFBII primer layer (purple) and without it (orange) between 1400 and 900 cm^{-1}.

© 2015 The Authors. Published by WILEY-VCH Verlag GmbH & Co. KGaA, Weinheim

Table 1. Water and dodecane contact angle values measured on commercial PS samples treated at pH 4 with HFBII, F10 or in sequence with both. The data are integrated with the calculation of the total surface free energy, and its polar and dispersive components.

Sample	Water CA [°]			Dodecane CA [°]			Surface energy [mJ m^{-2}]		
	Static CA	ACA	RCA	Static CA	ACA	RCA	Polar comp.	Dispersive comp.	Total
PS	88 ± 3	91 ± 2	84 ± 3	<10			2.6	44.6	47.2
PS + HFBII	58 ± 2	59 ± 2	56 ± 2	<10			13.0	42.4	55.4
PS + F10	95 ± 1	96 ± 1	94 ± 1	27 ± 3[a)]	28 ± 3[a)]	25 ± 3[a)]	0.4	47.1	47.5
PS + HFBII + F10	71 ± 3	71 ± 3	69 ± 3	58 ± 2	59 ± 2	57 ± 2	8.3	38.2	46.5
PS + HFBII + F10[b)]	85 ± 4	83 ± 4	85 ± 4	45 ± 2	46 ± 2	43 ± 3	8.6	37.3	45.9

[a)]Values resulting from the average on two drops. For three of five drops we found very small contact angles, well below the detection limit of the goniometer, suggesting a nonhomogenous coating; [b)]After the deposition of the two compounds at pH 4, the surface was washed with 10×10^{-3} M phosphate buffer (pH 7.4) and Milli-Q water.

the PS and PP surface coatings could not be studied by FT-IR because of overlaps between polymer vibrations and HFBII/PFPE coating peaks.

2.5. Characterization of the Coated Surfaces

The performance of the coating prepared via sequential immersion of the PS sheet in protein and F10 solutions at pH 4 was evaluated using static and dynamic CA measurements and estimation of the surface free energy using the Owens/Wendt method (**Table 1**; the complete dataset is presented in Table S4 of the Supporting Information). The untreated PS sheet exhibited a moderate surface energy (47 mJ m^{-2}), mostly originating from a dissipative component (45 mJ m^{-2}) and displayed rather hydrophobic behavior (88° water CA). As previously observed in model systems, the deposition of an HFBII monolayer increased the hydrophilicity of the PS surface, lowering its water contact angle to 58° and causing a clear increase in its polar surface energy component.

The subsequent coating with F10 resulted in a decrease of both the polar and dispersive components, while the water CA increased to 71°; although the total surface free energy was comparable to that of the pristine substrate, the different balance of its components clearly indicated the different chemical nature of the surface before and after the treatment. Although the most hydrophobic surface was observed to be that of the control samples treated only with F10 (95° water CA), their free surface energy composition appeared to be very similar to that of untreated PS.

Most importantly, a clear indication of the effectiveness of the protein primer layer was observed in the dodecane CAs, which indicated that a significant oleophilicity reduction could be obtained only on surfaces pretreated with HFBII (58° versus 27° CAs, however, it is important to observe that 27° is not a reliable number, since the surface exposed to F10 without the protein primer is not homogeneous. See the footnote in Table S4 of the Supporting Information for further details). These results confirmed that F10 alone adheres only poorly to the polymeric support and that the protein primer plays a key role in facilitating its adhesion to the PS surface, thus significantly reducing its oleophilic character. It is also important to remark that the results described here were obtained on samples which had been washed using rinsing solutions buffered both at pH 4 and at pH 7.4, which demonstrates that the overall coating is highly resistant to washing even at pH values higher than the ones used for the deposition. Furthermore, the low hysteresis observed between advancing CA (ACA) and receding CA (RCA) demonstrated that our method confers a stable oleophilicity reduction to the treated polymer surface.

Very similar results in terms of CAs and surface energies were observed for PP and LDPE samples functionalized using the same immersion procedure (see Tables S5 and S6 of the Supporting Information), demonstrating that, in these cases, F10 could significantly bind to the hydrophobic polymer surfaces only in the presence of the HFBII primer layer, which supports the general applicability of the method.

The PS samples prepared as above were also analyzed using AFM (**Figure 5**) for structural characterization. While the geometrical irregularity of the samples did not allow for precise visualization of the deposited films, some considerations can still be made by comparing the different surfaces using various parameters, such as the roughness (S_a), peak–peak height (S_y, height difference between highest and lowest pixel in the image), surface skewness (S_{sk}, height distribution asymmetry), and coefficient of kurtosis (S_{ku}, height distribution sharpness).[42] The complete set of parameters is reported in Table S7 of the Supporting Information.

A fairly smooth surface was consistently observed throughout the entire pristine PS sample (Figure 5a), which exhibited a quite low roughness (S_a = 1.23 nm), an average peak height of 5.62 nm and an S_y value of 12.34 nm. A skewness value close to zero (S_{sk} = 0.25 nm) indicated an essentially symmetrical distribution of peaks and valleys, and the general flatness of the surface was confirmed by the low coefficient of kurtosis (S_{ku} = 0.87).[43]

On the control sample prepared by immersion in F10 solution without the protein primer layer (Figure 5b), a few isolated peaks approximately 10 nm high are clearly visible. The low roughness (S_a = 0.81 nm), average peak height (5.60 nm), and S_y (13.44 nm) indicate that this sample was still very similar to the pristine PS; however the sparse new peaks caused a significant change in the coefficient of kurtosis (S_{ku} = 4.57). From an analysis of the images, these peaks generally corresponded to locations inside valley features; this result was confirmed by the skewness value, which was still close to zero (S_{sk} = –0.09 nm). This observation suggests a deposition mechanism based simply on mechanical adhesion[43] where a small amount of

 © 2015 The Authors. Published by WILEY-VCH Verlag GmbH & Co. KGaA, Weinheim

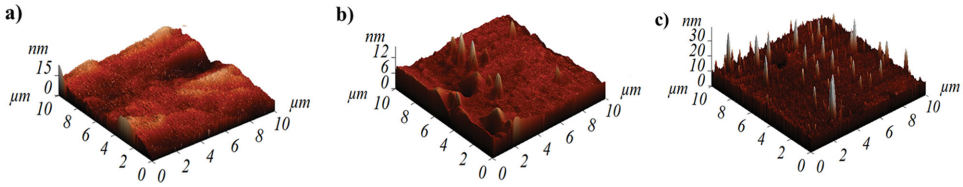

Figure 5. 3D reconstructions of AFM images of various PS surfaces, a) either pristine or treated by immersion in an F10 solution at pH 4 b) without or c) with a previously deposited HFBII primer layer. The area displayed in each image is 10 × 10 μm.

F10 remains stuck inside structural features already present in the pristine substrate.

However, the sample treated with sequential deposition of HFBII and F10 displayed a clearly different topography (Figure 5c). The roughness of the sample was nearly the same as that observed in the previous cases (S_a = 0.92 nm); however, the average peak height with respect to the base and S_y increased to 10.26 and 35.32 nm, respectively. The positive skewness (S_{sk} = 4.68 nm) and very large coefficient of kurtosis (S_{ku} = 43.73) indicated the formation of a multitude of aggregates 10–25 nm high with diameters that vary from tens to hundreds of nanometers on a flat surface. The observation of these aggregates is in agreement with those observed in the analogous QCM sensor model system (see Figure 3).

2.6. Oil Droplet Roll-Off Behavior of the Coated Polymer Surface

Finally, to further demonstrate the reduced oleophilicity attained by the PS surface coated with our sequential method of deposition of HFBII and F10, we assessed the rolling of dodecane and olive oil drops off the polymer surfaces using tilting experiments. The experiments were performed by depositing the oil drops on top of the different polymer surfaces tilted at a 30° angle. The oil drops slid rapidly away from the PS surface treated in sequence with HFBII and F10, without substantially wetting the treated polymer surface. Conversely, the oil drops remained as a film on both the pristine polymer and the control sample surface treated only with F10 (see **Figure 6** and the video available as the Supporting Information). This result further demonstrates that, by promoting the firm adhesion of the oleophobic fluoropolymer F10 to the apolar surface of PS, the HFBII primer layer endowed the hydrophobic PS surface with substantial and stable oil repellency features.

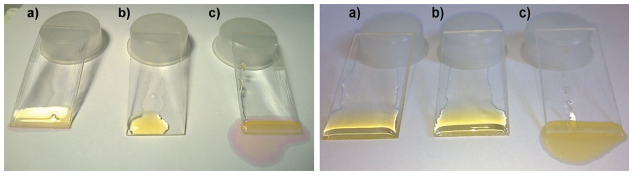

Figure 6. Tilting experiments performed using dodecane colored with nile red (left) and olive oil (right) drops. c) Oil drops roll off the surface treated with F10 in the presence of a previously deposited HFBII primer layer. Conversely, the oil drops remained as a film on the surfaces of a) both pristine PS and b) PS treated with F10 solution without previous HFBII coating.

3. Conclusions

In summary, we have presented a new, simple, and effective procedure for the fluoropolymer modification of poorly reactive (apolar) polymer surfaces based on the use of the protein hydrophobin HFBII as a nanosized primer layer. Hydrophobin changes the wettability of the apolar polymer surface to increase its hydrophilicity; its positively charged amino acid residues drive the self-assembly of anionic fluoropolymer surfactants. The self-assembly proceeds rapidly and spontaneously from aqueous solution and does not involve energy-intensive procedures, which makes it particularly sustainable from an environmental viewpoint. Our results demonstrate that biological adhesion proteins can be successfully used in materials applications. We have, in fact, applied this coating procedure to functionalize the surfaces of various apolar polymers, granting them substantial oil-repellency. Preliminary tests demonstrate that the same coating method can be applied to polydimethylsiloxane (PDMS), which is routinely used for the manufacture of microfluidic devices and microimprint stamps, and polymethylmethacrylate (PMMA), which is used to prepare medical implants. The application of the above-described fluoropolymer coating strategy to PDMS and PMMA to decrease the adhesion of hydrophobic molecules is currently under investigation in our laboratories and will be reported elsewhere.

4. Experimental Section

Materials and Methods: HFBII was produced using recombinant strains of *T. reesei*, purified by RP-HPLC, as described previously and lyophilized before use.[44–46] Fluorolink F10 (F10/A-ammonium salt, F10 in the text) was obtained from Solvay Specialty Polymers (Italy). The reagents (octadecylmercaptan, dodecane, ethylene glycol, diiodomethane) and solvents (*n*-hexane, 2-propanol, and methanol) were purchased from Sigma-Aldrich and used without further purification. Gold (QCX 301) and polystyrene-coated (QCX 305) QCM sensors were purchased from Biolin Scientific. Pure polystyrene, polypropylene and low-density polyethylene sheets were purchased from Goodfellow.

The experiments were performed at various pH values using 10 × 10^{-3} M buffer solutions of glycine/HCl (pH 3), sodium acetate (pH 4,5,6), and TRIS/HCl (pH 8); all of the buffer solutions contained 5% (v/v) 2-propanol.

Isoelectric Point Measurement: The theoretical isoelectric point of HFBII was previously determined to be pI = 6.7 using the program ProtParam.[47] Here, the pI of the protein was measured using a Zetasizer Nano-ZS instrument (Malvern, UK). HFBII was dissolved in 15 mL of Milli-Q water (0.1 mg mL^{-1}), and the starting pH was measured to be 4.6. The pH was adjusted using 10 × 10^{-3} M NaOH, and the zeta-potential was measured at 0.2 pH intervals. The experimentally determined pI value, obtained following two experimental replicates, was 5.8 (see Figure S1 and Table S1 of the Supporting Information).

© 2015 The Authors. Published by WILEY-VCH Verlag GmbH & Co. KGaA, Weinheim

QCM-D Experiments: A Q-Sense E4 instrument (Q-Sense) quartz crystal microbalance with dissipation monitoring (QCM-D) was used to measure the adsorbed mass of HFBII and F10 on octadecylmercaptan-coated self-assembled monolayers (SAM) on gold QCM crystals. The untreated crystals were first treated for 10 min in a UV/ozone chamber and then immersed at 75 °C in a $H_2O/NH_3/H_2O_2$ (5:1:1 v/v) mixture for 10 min. The sensors were rinsed thoroughly with Milli-Q water and dried with nitrogen. After a second 10 min treatment in the UV/ozone chamber, the sensors were functionalized overnight at RT by immersion in a 1×10^{-3} M octadecylmercaptan solution in *n*-hexane. Immediately before use, the SAM-coated crystals were washed with *n*-hexane and then with Milli-Q water, dried with nitrogen and mounted into the measurement chamber, which was maintained at 21 °C.

In a typical experiment, HFBII was dissolved in buffer solution at pH 3, 4, 5, 6, or 8 at a concentration of 0.1 mg mL^{-1}. After a stable baseline had been established, 500 µL of the protein sample was pumped through the measurement chambers using a flow of 100 µL min^{-1}. The sensors were then incubated for 30 min in zero-flow conditions, after which the surface was washed with the running buffer for 30–40 min to remove the excess protein. Subsequently, 500 µL of F10, dissolved into the same buffer solution to a final concentration of 1 mg mL^{-1}, was flowed through the chambers at a rate of 100 µL min^{-1}. The sensors were incubated for another 30 min in zero-flow conditions and then rinsed for 60–90 min using the running buffer. Control experiments were performed by exposing the sensor surfaces to F10 solutions without previous deposition of the HFBII layer with the same conditions as above. Dissipation values larger than zero imply that the adsorbed mass will not couple 100% to the oscillatory motion of the sensor. For this reason, the true adsorbed mass will be underestimated by the Sauerbrey equation; consequently, the adsorbed masses of HFBII and F10 were here estimated using the QTools software from the frequency and dissipation changes, applying the Voigt viscoelastic model to overtones 3, 5, 7, and 9. At the end of the measurement, all the sensors were briefly rinsed in Milli-Q water before contact angle and AFM measurements to remove buffer salt residues.

Hydrophobin and F10 Deposition on Hydrophobic Polymer Surfaces: The PS, PP, or LDPE sheets (approximately $50 \times 15 \times 1$ mm) were cleaned by 10 min sonication in methanol before use, rinsed thoroughly with Milli-Q water, and dried with nitrogen. The polymer samples were immersed vertically in a 0.1 mg mL^{-1} HFBII solution in pH 4 buffer for 45 min. The samples were then extracted, stirred for 20 s in clean buffer solution, and then immersed for 10 min in a vial containing clean buffer before repeating the same procedure using 1 mg mL^{-1} F10 in pH 4 buffer. To evaluate the coating resistance, phosphate buffer (10×10^{-3} M, pH 7.4) was used in the final rinsing of the PS-coated surfaces, replacing the use of the pH 4 buffer. All of the samples were rinsed with Milli-Q water and dried with nitrogen before characterization.

Following the same procedure, control experiments were performed using only an HFBII or F10 solution at pH 4.

ATR-FT-IR Spectroscopy Measurements: The IR spectra of HFBII, F10 and the treated/untreated supports were collected with a PerkinElmer Spectrum One FT-IR Spectrometer equipped with an ATR device. The spectra consisted of an average of 16 scans, with an acquisition range from 4000 to 450 cm^{-1} and a resolution of 2 cm^{-1}. The background was collected in air (for both HFBII and polymeric supports) or water (for F10). Magnifications and superimpositions of the collected spectra were performed using Origin 8 software.

Atomic Force Microscopy (AFM): Topography images of HFBII and F10 films adsorbed on QCM crystals coated with an octadecylmercaptan SAM layer were captured with a NanoScopeV Multimode8 AFM (E scanner, Bruker), and ScanAsyst-Air cantilevers (Bruker, f_0 = 50–90 kHz, k = 0.4 N m^{-1}) were used in all measurements. All of the images were recorded in the ScanAsyst mode in air with a 1 Hz scan rate. The images were only flattened to remove possible tilt in the image data, and no further processing was performed. The NanoScope Analysis software (Bruker) was used for image processing and analysis. RMS roughness (R_q) values were calculated as an average of three images from the same sample.

The atomic force microscope analyses of the PS sheets were performed using an AFM Solver Pro (NT-MDT) instrument. The measured areas (10 µm × 10 µm) were scanned at a rate of 0.6 Hz with an NT-MDT cantilever (f_0 = 190–354 Hz; k = 5.5–22.5 N m^{-1}). The output data were collected using the NOVA SPM software.

Contact Angle and Surface Energy Measurements: The contact angles of all of the solid samples with different solvents were determined using an OCA 15 PLUS instrument (Dataphysics) using droplet volumes of 4 µL for Milli-Q water and 2 µL for dodecane, ethylene glycol, and diiodomethane. Advancing and receding contact angles were measured through the tilting plate method. The average contact angles (Elliptic method) were calculated from a series of five independent measurements by the SCA20 software. The surface energy was calculated from the contact angle values with water, ethylene glycol, and diiodomethane using the Owens–Wendt method.

Tilting Experiments: PS sheets, either untreated or treated with F10 in the presence or absence of the hydrophobin primer layer as described above, were tilted at angles of 30°, and 200 µL of olive and dodecane oils was deposited on the top edge. Observing the behavior of the oil droplets, which either stuck to or slid off the surfaces, provided an indication of the degree of oil repellency of the samples.

Supporting Information

Supporting Information is available from the Wiley Online Library or from the author.

Acknowledgements

The authors thank James Evans from VTT for preparing clean gold chip for the AFM imaging and Riccardo Carzino from IIT-NAPH Genova for helpful discussions. Financial support from the Academy of Finland (#126572 and #260565) and from the Cariplo Foundation (project S2N) is acknowledged. Solvay Specialty Polymers (Italy) is also acknowledged for the gift of a sample of Fluorolink F10.

Received: April 4, 2015
Revised: June 12, 2015
Published online:

[1] A. P. Kharitonov, R. Taege, G. Ferrier, V. V. Teplyakov, D. A. Syrtsova, G. H. Koops, *J. Fluorine Chem.* **2005**, *126*, 251.
[2] A. P. Kharitonov, *J. Fluorine Chem.* **2000**, *103*, 123.
[3] D. Anton, *Adv. Mater.* **1998**, *10*, 1197.
[4] H. Wang, J. Fang, T. Cheng, J. Ding, L. Qu, L. Dai, X. Wang, T. Lin, *Chem. Commun.* **2008**, *7*, 877.
[5] S. Turri, R. Valsecchi, M. Viganò, M. Levi, *Polym. Bull.* **2009**, *63*, 235.
[6] H. Jenewein, D. L. Kerbow, (E. I. Du Pont de Nemours and Company) *US 5576106 A*, **1996**.
[7] T. J. Blong, E. E. Parsonage, (Dyneon LLC) *US 6117508 A*, **2000**.
[8] A. Di Gianni, R. Bongiovanni, A. Priola, S. Turri, *Int. J. Adhes. Adhes.* **2004**, *24*, 513.
[9] Y. Yoon, D. W. Lee, J. B. Lee, *J. Micromech. Microeng.* **2012**, *22*, 035012/1.
[10] Q. Cheng, K. Komvopoulos, *J. Phys. D: Appl. Phys.* **2012**, *45*, 095401/1.
[11] P. Favia, R. d'Agostino, *Surf. Coat. Technol.* **1998**, *98*, 1102.
[12] J. P. Youngblood, T. J. McCarthy, *Macromolecules* **1999**, *32*, 6800.
[13] J. Shimada, M. Hoshino, *J. Appl. Polym. Sci.* **1975**, *19*, 1439.
[14] B. A. Butruk, P. A. Ziętek, T. Ciach, *Cent. Eur. J. Chem.* **2011**, *9*, 1039.
[15] Solvay Specialty Polymers, *Fluorolink and Solvera Products*. Available from: http://www.solvaysites.com/sites/solvayplastics/EN/specialty_polymers/Fluorinated_Fluids/Pages/Fluorinated_Fluids.aspx (accessed: February 2014).

 © 2015 The Authors. Published by WILEY-VCH Verlag GmbH & Co. KGaA, Weinheim

[16] R. A. Ryntz, *JCT Res.* **2005**, *2*, 350.
[17] D. Wang, R. D. Oleschuk, J. H. Horton, *Langmuir* **2008**, *24*, 1080.
[18] P. Sun, J. H. Horton, *Appl. Surf. Sci.* **2013**, *271*, 344.
[19] R. Milani, M. Gleria, A. Sassi, R. De Jaeger, A. Mazzah, L. Gengembre, M. Frere, C. Jama, *Chem. Mater.* **2007**, *19*, 4975.
[20] M. B. Linder, G. R. Szilvay, T. Nakari-Setälä, M. E. Penttilä, *FEMS Microbiol. Rev.* **2005**, *29*, 877.
[21] J. Hakanpää, A. Paananen, S. Askolin, T. Nakari-Setälä, T. Parkkinen, M. E. Penttilä, M. B. Linder, J. Rouvinen, *J. Biol. Chem.* **2004**, *279*, 534.
[22] G. R. Szilvay, A. Paananen, K. Laurikainen, E. Vuorimaa, H. Lemmetyinen, J. Peltonen, M. B. Linder, *Biochemistry* **2007**, *46*, 2345.
[23] M. B. Linder, *Curr. Opin. Colloid Interface Sci.* **2009**, *14*, 356.
[24] J. G. H. Wessels, *Annu. Rev. Phytopathol.* **1994**, *32*, 413.
[25] M. B. Linder, G. R. Szilvay, T. Nakari-Setälä, H. Soderlund, M. E. Penttilä, *Protein Sci.* **2002**, *11*, 2257.
[26] Z. X. Zhao, H. C. Wang, X. Qin, X. S. Wang, M. Q. Qiao, J. I. Anzai, Q. Chen, *Colloids Surf. B* **2009**, *71*, 102.
[27] Z. Wang, Y. Huang, S. Li, H. Xub, M. B. Linder, M. Q. Qiao, *Biosens. Bioelectron.* **2010**, *26*, 1074.
[28] Z. X. Zhao, M. Q. Qiao, F. Yin, B. Shao, B. Y. Wu, Y. Y. Wang, X. S. Wang, X. Qin, S. Li, L. Yu, Q. Chen, *Biosens. Bioelectron.* **2007**, *22*, 3021.
[29] Y. Corvis, A. Walcarius, R. Rink, N. T. Mrabet, E. Rogalska, *Anal. Chem.* **2005**, *77*, 1622.
[30] J. Hakanpää, M. B. Linder, A. Popov, A. Schmidt, J. Rouvinen, *Acta Crystallogr. D* **2006**, *D62*, 356.
[31] A. Zaggia, B. Ameduri, *Curr. Opin. Colloid Interface Sci.* **2012**, *17*, 188.
[32] M. A. Guerra, K. Hintzer, M. Jurgens, H. Kaspar, A. R. Maurer, G. Moore, Z. M. Qiu, J. F. Schulz, W. Schwertfeger, T. Zipplies, (3M Innovative Properties Company), *US20070276103 A1*, **2007**.
[33] M. D. Evans, K. M. McLean, T. C. Hughes, D. F. Sweeney, *Biomaterials* **2001**, *22*, 3319.
[34] D. F. Sweeney, A. Vannas, T. C. Hughes, M. D. Evans, K. M. McLean, R. Z. Xie, V. K. Pravin, R. K. Prakasam, *Vision CRC Inlay Team, Clin. Exp. Optom.* **2008**, *91*, 56.
[35] R. Bongiovanni, A. Nelson, A. Vitale, E. Bernardi, *Thin Solid Film* **2012**, *520*, 5627.
[36] J. Hakanpää, G. R. Szilvay, H. Kaljunen, M. Maksimainen, M. B. Linder, J. Rouvinen, *Protein Sci.* **2006**, *15*, 2129.
[37] M. S. Grunér, G. R. Szilvay, M. Berglin, M. Lienemann, P. Laaksonen, M. B. Linder, *Langmuir* **2012**, *28*, 4293.
[38] G. R. Szilvay, K. Kisko, R. Serimaa, M. B. Linder, *FEBS Lett.* **2007**, *581*, 2721.
[39] K. Sulak, M. Wolszczak, A. Chittofrati, E. Szajdzinska-Pietek, *J. Phys. Chem. B* **2005**, *109*, 799.
[40] C. Gambi, R. Giordano, A. Chittofrati, R. Pieri, P. Baglioni, J. Teixeira, *J. Phys. Chem. B* **2005**, *109*, 8592.
[41] K. Sulak, M. Wolszczak, A. Chittofrati, E. Szajdzinska-Pietek, *J. Photochem. Photobiol. A* **2007**, *191*, 1.
[42] J. Peltonen, M. Järn, S. Areva, M. Linden, J. B. Rosenholm, *Langmuir* **2004**, *20*, 9428.
[43] R. Leach, *Fundamental Principles of Engineering Nanometrology*, Elsevier, Burlington, MA **2010**.
[44] M. J. Bailey, S. Askolin, N. Hörhammer, M. Tenkanen, M. B. Linder, M. Penttilä, T. Nakari-Setälä, *Appl. Microbiol. Biotechnol.* **2002**, *58*, 721.
[45] A. Paananen, E. Vuorimaa, M. Torkkeli, M. E. Penttilä, M. Kauranen, O. Ikkala, H. Lemmetyinen, R. Serimaa, M. B. Linder, *Biochemistry* **2003**, *42*, 5253.
[46] M. B. Linder, K. Selber, T. Nakari-Setälä, M. Qiao, M. R. Kula, M. Penttilä, *Biomacromolecules* **2001**, *2*, 511.
[47] J. M. Walker, *The Proteomics Protocols Handbook*, Humana Press, Totowa, NJ **2005**, p. 571.

© 2015 The Authors. Published by WILEY-VCH Verlag GmbH & Co. KGaA, Weinheim